Soret Effect on the Radiative MHD Free Convective Viscous Flow over an Inclined Plate Embedded in a Porous Medium.

M. Rajaiah, Dr.A. Sudhakaraiah

Abstract— **The present study deals with the combined effects of Soret and chemical reaction on the radiative MHD free convection flow of an electrically conducting incompressible viscous fluid over an inclined plate embedded in a porous medium is studied. The impulsively started plate with variable temperature and mass diffusion is considered. The dimensionless governing partial differential equations have been solved numerically and expressions for velocity, temperature and concentration profile are obtained. They satisfy all imposed initial and boundary conditions and can be reduced, as special cases, to some known solutions from the literature. Expressions for skin friction, Nusselt number and Sherwood number are also obtained. The effects of pertinent parameters on velocity, temperature and concentration profiles are graphically displayed where as the variations in skin friction, Nusselt number and Sherwood number are shown through tables.**

Index Terms— **Soret number (Sr), Inclined plate, MHD free convective, Viscous flow, Chemical reaction**

I. INTRODUCTION

The conjugate effects of heat and mass transfer occurs as a result of combined buoyancy effects of thermal and mass diffusion which essentially plays an important role in Geophysics, Aeronautics and Chemical Engineering. Guo Z, Sung Hj [1] studied the conjugate effect of heat and mass transfer in metal hydride beds in the hydriding process which is useful in food drying, food processing and polymer production. The conjugate phenomenon of heat and mass transfer either analytically or numerically gained a considerable amount of interest in recent years and extensive research work is done on account of this [2 –5]. Bhuvaneswari M et al. [6] studied an exact analysis of radiation convective flow heat and mass transfer over an inclined plate in a porous medium. Kandasamy R et al. [7] analysed the Lie group analysis for the effect of temperature-dependent fluid viscosity with thermophoresis and chemical reaction on MHD free convective heat and mass transfer over a porous stretching surface in the presence of heat source/sink.

Ahmed N and Sarmah H.K [8] investigated the thermal radiation effect on a transient MHD flow with mass transfer past an impulsively fixed infinite vertical plate. Rajput and Kumar [9] thoroughly studied the MHD flow past an impulsively started vertical plate with variable temperature and mass diffusion. They used the Laplace transform method to find the exact solutions for velocity, temperature and concentration. In a subsequent year Rajput and Kumar [10] extended by taking the thermal radiation effect. Ahmad [11] studied MHD transient free convection and mass transfer flow of a viscous, incompressible and electrically conducting fluid in the presence of thermal diffusion and thermal radiation. He obtained exact solutions for velocity, temperature, and concentration using the Laplace transforms method. Osman et al. [12] studied analytically the thermal radiation and chemical reaction effects on unsteadyMHD free convection flow in a porous medium with heat source/ sink.

By taking the porous medium effect, Sami et al. [13] provided an exact analysis to the study of the magnetohydrodynamic free convection flow of an incompressible viscous fluid past an infinite vertical oscillating plate with uniform heat flux. In other investigation, Sami et al. [14] studied the MHD free convection flow in a porous medium with thermal diffusion and ramped wall temperature. They obtained exact dimensionless solutions of momentum and energy equations, under Boussinesq approximation using the Laplace transforms. Magyari E, Pantokratoras A [15] gave a note on the effect of thermal radiation in the linearized Rosseland approximation on the heat transfer characteristics of various boundary layer flows.

Ziyauddin and Kumar [16] studied the radiation effects on unsteady MHD natural convection flow in a porous medium with conjugate heat and mass transfer past a moving inclined plate in the presence of chemical reaction, variable temperature and mass diffusion. They used an explicit finite difference method to solve the coupled linear partial differential equations numerically, and the results are graphically displayed. Unfortunately, in this work the plate is not porous as the authors mentioned in the paper. On the other hand the numerical solutions of the free convection problems are more convenient and easy to handle as compare to exact solutions. Muthucumaraswamy and Janakiraman[17] obtained exact solutions for the MHD flow of viscous optically thin fluid past a vertical flat plate in a non-porous medium. They considered uniform heat and variable mass transfer.

Farhad Ali [18] presented an exact analysis of combined effects of radiation and chemical reaction on the MHD free convection flow of an electrically conducting incompressible viscous fluid over an inclined plate embedded in a porous medium. The impulsively started plate with variable temperature and mass diffusion is considered. The dimensionless momentum equation coupled with the energy and mass diffusion equations are analytically solved using the Laplace transform method.

The aim of this study is to present an analysis of combined effects of Soret and viscosity the radiative MHD free

M.Rajaiah presently working professor an HOD department of Humanities and Sciences ,Audisankara College of Engineering &Technology ,Gudur, Nellore, AP, India

convection flow of an electrically conducting incompressible viscous fluid over an inclined plate embedded in a porous medium. The impulsively started plate with variable temperature and mass diffusion is considered. The dimensionless momentum equation coupled with the energy and mass diffusion equations are numerically solved and expressions for velocity, temperature and concentration fields are obtained. They satisfy all imposed initial and boundary conditions and can be reduced, as special cases, to some known solutions from the literature. Expressions for skin friction, Nusselt number and Sherwood number are also obtained. Finally, the effects of pertinent parameters on velocity, temperature and concentration profiles are graphically displayed whereas the variations in skin friction, Nusselt number and Sherwood number are presented clearly through tables.

II. Formulation of the Problem

A radiative MHD free convection flow of an electrically conducting incompressible viscous fluid over an inclined plate embedded in a porous medium is considered under the following assumptions

1. The plate is started impulsively with variable temperature and the mass diffusion is considered
2. The x^* - axis is taken along the plate with the angle of inclination (α) to the vertical and the y^*- axis is taken normal to the plate.
3. The viscous fluid is taken to be electrically conducting and fills the porous half space $y^* > 0$.
4. A uniform magnetic field of strength B_o is applied in the y^*-direction transversely to the plate. The applied magnetic field is assumed to be strong enough so that the induced magnetic field due to the fluid motion is weak and can be neglected.
5. According to Cramer and Pai[5], this assumption is physically justified for partially ionized fluids and metallic liquids because of their small magnetic Reynolds number. Since there is no applied or polarization voltage imposed on the flow field, the electric field due to polarization of charges is zero.
6. Initially, both the fluid and the plate are at rest with constant temperature T_∞^* and constant concentration C_∞^*. At time $t^* = 0^+$, the plate is given a sudden jerk, and the motion is induced in the direction of flow against the gravity with uniform velocity u_0.The temperature and concentration of the plate is raised linearly with respect to time.
7. The fluid is thick gray absorbing-emitting radiation but non–scattering medium.
8. Since the plate is infinite in the (x^*, z^*) plane, all physical variables are functions of y^* and t* only.

The physical model and the coordinate system is shown in the following figure

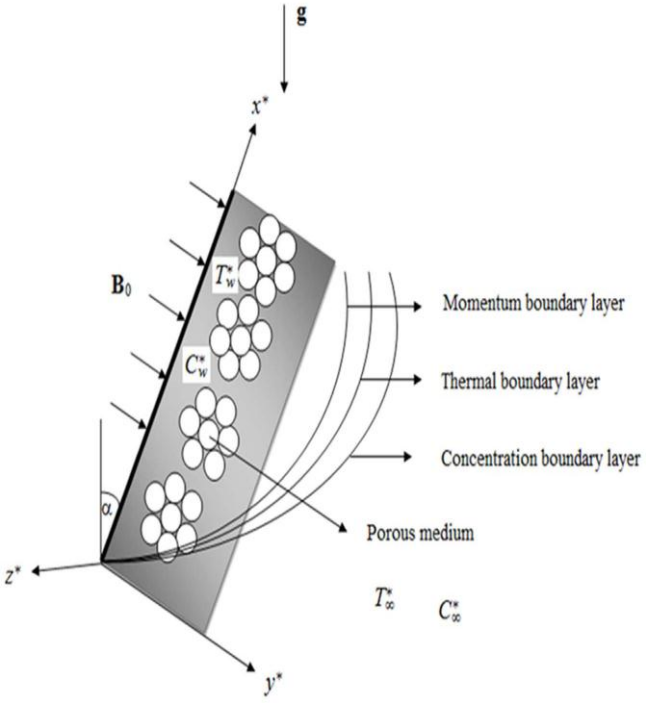

In view of the above assumptions, as well as of the usual Boussineq's approximation, the governing equations reduce

$$\frac{\partial v'}{\partial t'} = 0 \tag{1}$$

$$\frac{\partial u^*}{\partial t^*} = \frac{\partial^2 u^*}{\partial y^{*2}} - \left(\frac{\sigma B_0^2}{\rho} + \frac{\nu}{K^*}\right) u^* + g\,\beta_T \left(T^* - T_\infty^*\right) Cos(\alpha) + g\,\beta_C \left(C^* - C_\infty^*\right) Cos(\alpha) \tag{2}$$

$$\rho C_P \frac{\partial T^*}{\partial t^*} = \kappa \frac{\partial^2 T^*}{\partial y^{*2}} + \mu \left(\frac{\partial u^*}{\partial y^*}\right)^2 - \frac{\partial q_r}{\partial y^*} \tag{3}$$

$$\frac{\partial C^*}{\partial t^*} = D \frac{\partial^2 C^*}{\partial y^{*2}} - K_1 \left(C^* - C_\infty^*\right) + \frac{D\,\kappa_T}{T_m} \frac{\partial^2 T^*}{\partial y^{*2}} \tag{4}$$

The initial and boundary conditions are

$$u^*\left(y^*,\,0\right)=0,\quad T^*\left(y^*,\,0\right)=T_\infty^*,\quad C^*\left(y^*,\,0\right)=C_\infty^*\quad y^*>0$$

$$u^*\left(\infty,\,t^*\right)=0,\quad T^*\left(\infty,\,t^*\right)=T_\infty^*,\quad C^*\left(\infty,\,t^*\right)=C_\infty^*\quad t^*>0 \tag{5}$$

Following Magyari and Pantokratoras [15] the Rosseland's approximation for radiative flux (q_r) is adopted

i.e. $$q_r=-\frac{4\sigma_0}{3\chi}\frac{\partial T^{*4}}{\partial y^*} \tag{6}$$

$$\left.\begin{aligned} &u^*\left(0,\;t^*\right)=u_0,\\ \text{and}\quad &T^*\left(0,\;t^*\right)=T_\infty^*+\left(T_w^*-T_\infty^*\right)At^*,\\ &C^*\left(0,\;t^*\right)=C_\infty^*+\left(C_w^*-C_\infty^*\right)At^* \end{aligned}\right\}\quad t^*>0 \tag{7}$$

The temperature differences within the flow are assumed to be so small and T^{*4} can be expressed as a linear function of the temperature. This is accomplished by expanding T^{*4} in a Taylor's series about T_∞^* and neglecting higher order terms to get

$$T^{*4}\approx 4T_\infty^{*3}T-3T_\infty^{*4} \tag{8}$$

Substituting equations (6) and (8) in (3) to get

$$\rho C_P\frac{\partial T^*}{\partial t^*}=\kappa\frac{\partial^2 T^*}{\partial y^{*2}}+\mu\left(\frac{\partial u^*}{\partial y^*}\right)^2-\kappa\left(1+\frac{16\sigma_0 T_\infty^{*3}}{3\chi\kappa}\right)\frac{\partial^2 T^*}{\partial y^{*2}} \tag{9}$$

Introducing the non–dimensional quantities

$$u=\frac{u^*}{u_0}\qquad y=\frac{u_0}{\nu}y^*\qquad t=\frac{{v_0}^2}{\nu}t^*\qquad A=\frac{{u_0}^2}{\nu}\qquad \gamma=\frac{K_1\nu}{{u_0}^2}$$

$$\theta=\frac{T^*-T_\infty^*}{T_w^*-T_\infty^*}\qquad \phi=\frac{C^*-C_\infty^*}{C_w^*-C_\infty^*}\qquad K=\frac{{u_0}^2}{\nu^2}K^* \tag{10}$$

Into the governing equations and initial and boundary conditions to get the governing equations with the corresponding initial and boundary conditions in the non – dimensional form are

$$\frac{\partial u}{\partial t}=\frac{\partial^2 u}{\partial y^2}-\left(M+\frac{1}{K}\right)u+Gr\;\theta Cos(\alpha)+Gc\,\phi Cos(\alpha) \tag{11}$$

$$\frac{\partial\theta}{\partial t}=\frac{1}{\Pr}(1+N)\frac{\partial^2\theta}{\partial y^2}+Ec\left(\frac{\partial u}{\partial y}\right)^2 \tag{12}$$

$$\frac{\partial\phi}{\partial t}=\frac{1}{Sc}\frac{\partial^2\phi}{\partial y^2}-\gamma\,\phi+Sr\frac{\partial^2\theta}{\partial y^2} \tag{13}$$

$$\begin{aligned} &t\le 0\;;\quad u(y,t)=0,\quad \theta(y,t)=0,\quad \phi(y,t)=0\qquad y>0\\ &t>0\;;\quad u(0,\,t)=1,\quad \theta(0,\,t)=t,\quad \phi(0,\,t)=t\qquad y=0\\ &\qquad\quad u(y,\,t)\to 0,\quad \theta(y,\,t)\to 0,\quad \phi(y,\,t)\to 0\quad y\to\infty \end{aligned} \tag{14}$$

III. Finite Difference Scheme

Since exact or approximate solutions are not possible for this set of equations, an implicit finite difference method is used to solve the governing equations subject to the respective initial and boundary conditions. Using the finite difference scheme, the governing equations with the corresponding boundary conditions become

$$\frac{u(i,\ j+1)\ -\ u(i,\ j)}{\Delta t}\ =\ \frac{1}{2}Gr\,(\theta(i,\ j)+\theta(i,\ j+1))\ Cos(\alpha)\ +\ \frac{1}{2}Gc\,(\phi(i,\ j)+\phi(i,\ j+1))\ Cos(\alpha)$$
$$-\ \frac{1}{2}\left(M\ +\ \frac{1}{K}\right)(u(i,\ j)+u(i,\ j+1))$$
$$+\ \frac{u(i+1,\ j)\ -\ 2u(i,\ j)\ +\ u(i-1,\ j)+u(i+1,J+1)-2u(i,j+1)+u(i-1,j+1)}{2\Delta y^2} \quad (15)$$

$$\frac{\theta(i,\ j+1)\ -\ \theta(i,\ j)}{\Delta t}\ =\ Ec\left[\ \frac{u(i+1,\ j)\ -\ u(i,\ j)+u(i+1,j+1)-u(i,j+1)}{2\Delta y}\ \right]^2$$
$$+\left(\frac{1\ +\ N}{\Pr}\right)\ \frac{\theta(i+1,\ j)\ -\ 2\theta(i,\ j)\ +\ \theta(i-1,\ j)+\theta(i+1,j+1)-2\theta(i.j+1)+\theta(i-1,j+1)}{2\Delta y^2} \quad (16)$$

$$\frac{\phi(i,\ j+1)\ -\ \phi(i,\ j)}{\Delta t}\ =\ -\ \frac{1}{2}\gamma\ (\phi(i,\ j)+\phi(i,j+1))$$
$$+\frac{1}{Sc}\ \frac{\phi(i+1,\ j)\ -\ 2\phi(i,\ j)\ +\ \phi(i-1,\ j)+\phi(i+1,j+1)-2\phi(i,j+1)+\phi(i-1,j+1)}{2\Delta y^2} \quad (17)$$
$$+\ Sr\ \frac{\theta(i+1,\ j)\ -\ 2\theta(i,\ j)\ +\ \theta(i-1,\ j)+\theta(i+1,j+1)-2\theta(i,j+1)+\theta(i-1,j+1)}{2\Delta y^2}$$

$$j \le 0\ ;\ u(i,\ 0) = 0,\quad \theta(i,\ 0) = 0,\quad \phi(i,\ 0) = 0\quad for\ i > 0 \quad (18)$$

$$j > 0\ \begin{cases} u(0,\ j) = 1,\quad \theta(0,\ j) = j,\quad \phi(0,\ j) = j\quad i = 0 \\ u(i,\ j) \to 0,\ \theta(i,\ j) \to 0,\quad \phi(i,\ j) \to 0\quad i \to \infty \end{cases}$$

The suffixes, *i* corresponds to *y* and *j* corresponds to *t* and $\Delta t = t(i+1) - t(i)$ and $\Delta y = y(j+1) - y(j)$. The computations were carried out for different values of the various physical parameters.

The Skin – friction coefficient or the shear stress at the wall is given by

$$\tau\ =\ -\left[\ \frac{\partial u(y,\ t)}{\partial y}\ \right]_{y\ =\ 0} \quad (19)$$

The rate of heat transfer in terms of the Nusselt number is

$$Nu\ =\ -\left[\ \frac{\partial \theta(y,\ t)}{\partial y}\ \right]_{y\ =\ 0} \quad (20)$$

The rate of mass transfer in terms of Sherwood number is

$$Sh\ =\ -\left[\ \frac{\partial \phi(y,\ t)}{\partial y}\ \right]_{y\ =\ 0} \quad (21)$$

IV. Discussion of Results

The numerical solutions for the velocity, temperature, and mass diffusion are computed for various physical parameters such as Hartmann number (M), Eckert number (Ec), Prandtl number (Pr), time (*t*), and Schmidt number (Sc), etc. The skin – friction, the rate of heat transfer in terms of the Nusselt number (Nu), and the rate of mass transfer in terms of the Sherwood number (Sh) are also derived in terms of the given system parameters. The results are shown in graphs and tables.

The velocity profiles are discussed through graphs 1 to 6 for various parameters such as Hartmann number (M), thermal Grashoff number (Gr), the Solutal

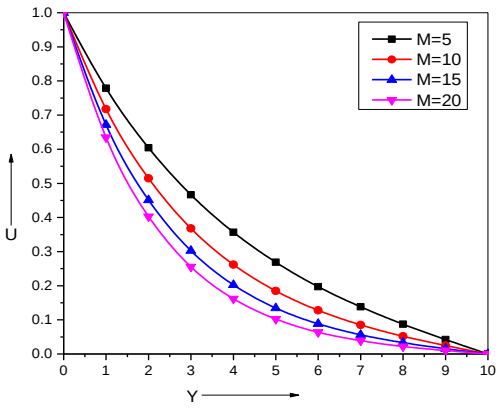

Fig.1
Variation of velocity profiles for different values of M

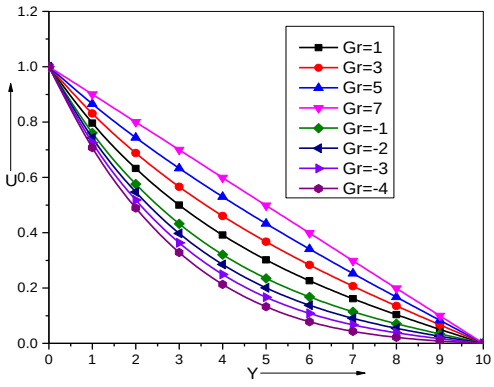

Fig. 2 Velocity profiles for different values of Gr

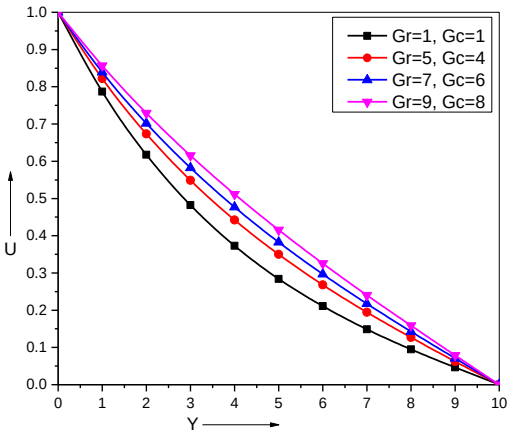

Fig. 3
Variation of velocity profiles for different values of Gr and Gc

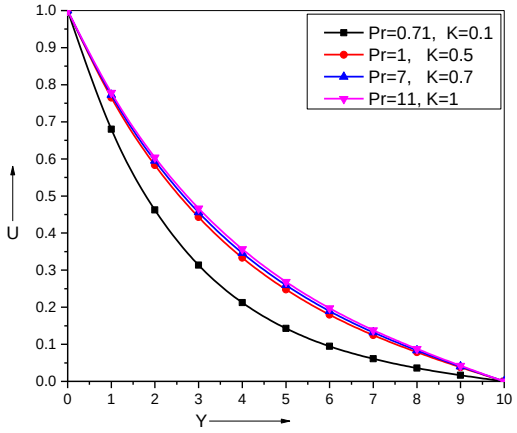

Fig. 4
Variation of velocity profiles for different values of Pr and K

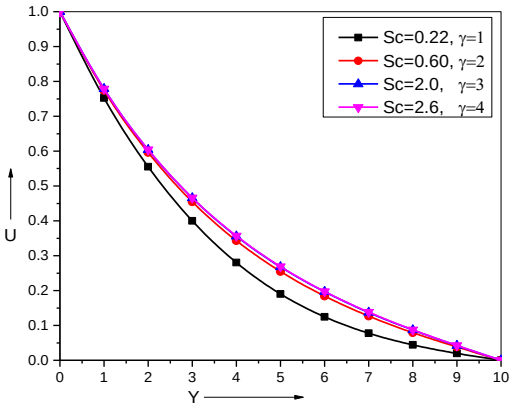

Fig. 5
Variation of velocity profiles for different values of Sc, **γ** and **α**

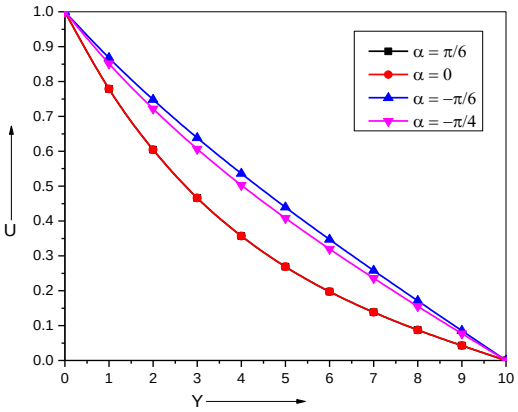

Fig. 6
Variation of velocity profiles with inclination α

The effect of Magnetic parameter M on the velocity profile is presented in figure 1. It is seen that the velocity decreases as the magnetic parameter M is increases. Physically, it is justified because the application of transverse magnetic field always results in a resistive type force called Lorentz force which is similar to drag force and tends to resist the fluid motion, finally reducing its velocity.

The variation of velocity distribution to the thermal Grashoff number is discussed in the figure 2. The thermal Grashoff number is the relative effect of the thermal buoyancy force to the viscous hydrodynamic force in the boundary layer. The positive values of Grashoff number indicates the cooling of the plate. The rise in the velocity is observed due to the enhancement of the thermal buoyancy force. As thermal buoyancy increases, the velocity increases rapidly near the plate and gradually decreases to free stream velocity. With the decrease of the thermal Grashof number i.e Gr<0, from figure, an opposite behavior is observed.

The combined effect of Grashof number (Gr) and the Solutal Grashof number (Gc) is shown in the figure 3. Similar to the thermal Grashoff number, the Solutal Grashoff number effect is also to increase in the velocity. The rise in the velocity distribution with the increase of Solutal Grashof number observed in the figure and also the gradual decrease in the boundary layer.

In the figure 4, the combined effect of Prandtl number (Pr) and the permeability parameter (K) is given. Physically, it is true due to the fact that an increase in Prandtl number increases the viscosity of the fluid, becomes thick and consequently leads to a decrease in the velocity. But increase in permeability increases the size of the pores which

influences the flow to be fast so that the velocity increases with the increase of Pr and K.

The variation of velocity distribution with the physical parameters Schmidt number (Sc) and the chemical reaction parameter (γ) is observed from the figure 5. With the increase of Sc and γ, the velocity rises but decreases gradually in the boundary layer and reaches a steady state. This effect can be seen from the figure. It is noticed from the figure 6 that the velocity increases sharply as the inclination decreases.

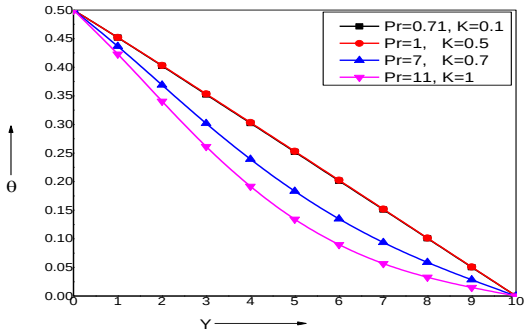

Fig. 7
Variation of temperature profiles for different values of Pr and K

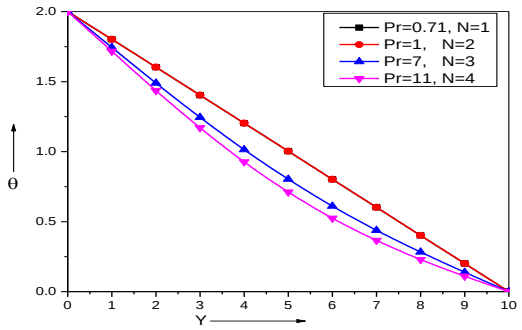

Fig. 8
Variation of temperature profiles for different values of Pr and N when t=2

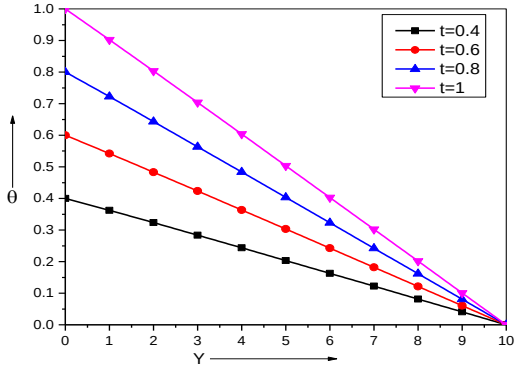

Fig. 9
Variation of temperature profiles for different values of t when Pr=0.71 and N=1

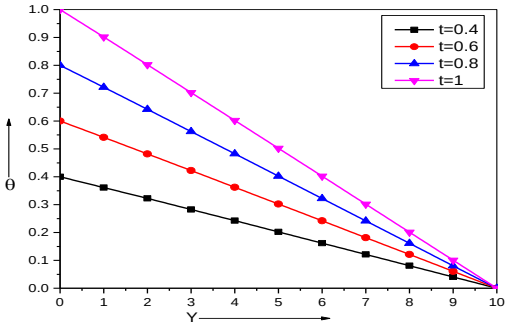

Fig. 10
Variation of temperature profiles for different values of t when Sc=2 and γ=1

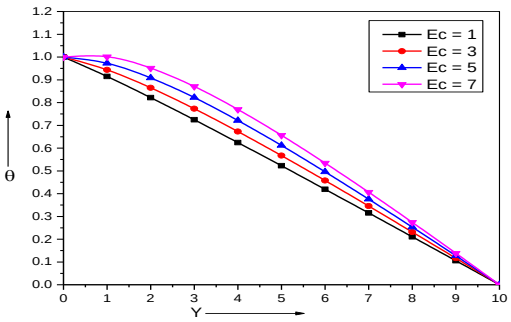

Fig. 11
Variation of temperature profiles for different values of Ec

Figure 7 depicts the influence of Prandtl number (Pr) and permeability parameter (K) on the temperature. Four different values of Prandtl number namely Pr~0:71, 1, 7, and 11 corresponding to air, electrolyte, water and lubricants respectively are chosen. It is mainly observed that temperature decreases with increasing Pr. It is interesting to note that a comparison of curves shows that the temperature falls more rapidly for water in comparison to air. A similar behaviour is also expected due to the fact that increasing Pr means the increasing viscous nature of a fluid. For smaller values of Prandtl number fluids possess high thermal conductivity and heat diffuses away from the surface faster than at higher values of Prandtl number. Thus the boundary layer becomes thicker and consequently the temperature decreases when Pr is increased. Furthermore, the temperature profiles for increasing values of permeability parameter K indicate a decreasing behaviour as shown in the figure.

The temperature profiles for increasing values of radiation parameter (N) and Prandtl number (Pr) is shown in the figure 8.It is expected to observe an increase in the temperature but with the simultaneous increase in the Prandtl number decreases the temperature. This can be seen from the figure.

Figures 9 and 10 is plotted to show the effect of the dimensionless time t on the temperature when $\Pr = 0.71$ and $N = 1$ and $Sc = 2$ and $\gamma = 1$. Four different values of time $t \cong 0.4,\ 0.6,\ 0.8,$ and 1.0 are chosen. Obviously, the temperature increases with increasing time.

The rise of the temperature distribution with the Eckert number is shown in the figure 11. The temperature increases with the respective increase in the Eckert number. The temperature increases slightly near the plate but decreases sharply away from the plate i.e. with the increase in the boundary
layer.

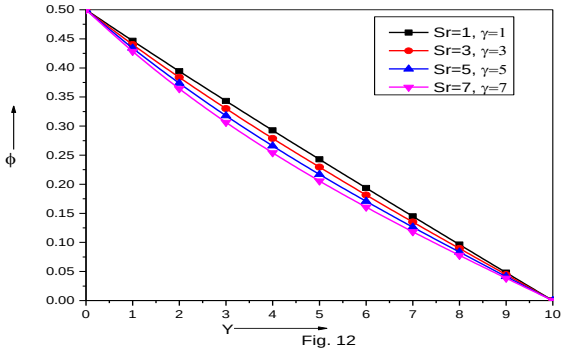

Fig. 12
Variation of Concentration profiles for different values of Sr and γ

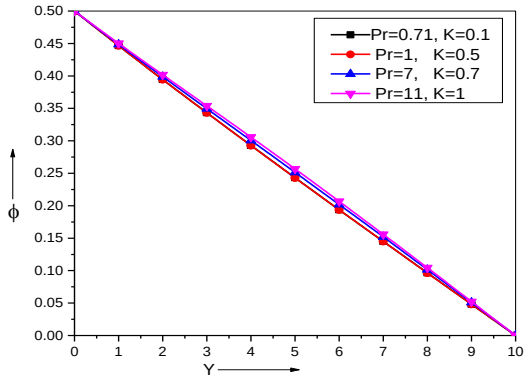

Fig. 13
Variation of Concentration profiles for different values of Pr and K

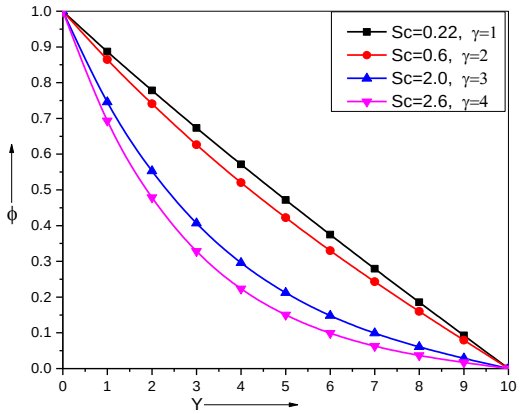

Fig. 14
Variation of Concentration profiles for different values of Sc, **γ** and **α**

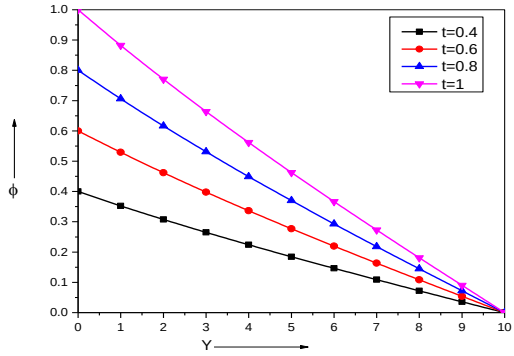

Fig. 15.1
Variation of Concentration profiles for different values of t when Pr=0.71 and N=1

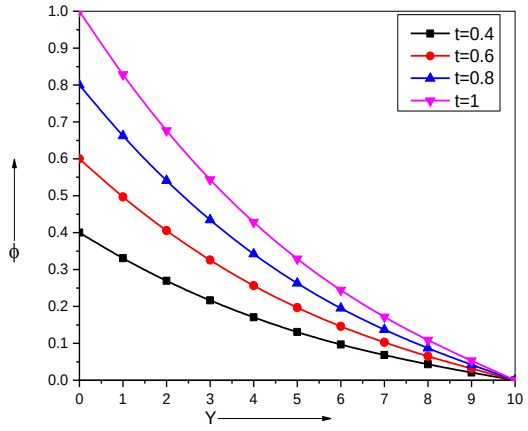

Fig. 15.2
Variation of Concentration profiles for different values of t when Sc=2 and **γ**=1

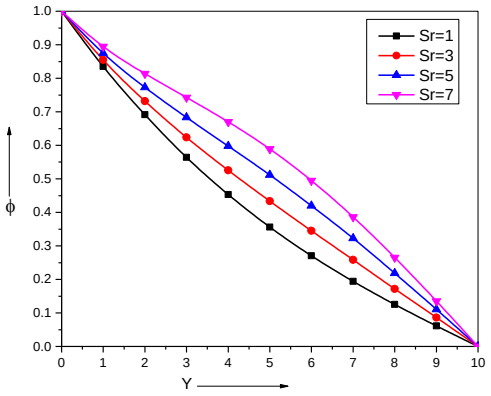

Fig.17
Variation of Concentration profiles for different values of Sr

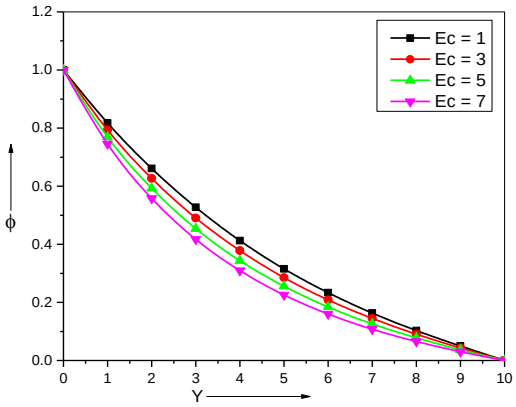

Fig. 18
Variation of Concentration profiles for different values of Ec

Figure 12 shows the influence of the Soret number (Sr) and chemical reaction parameter (γ) on the concentration profiles. The rise in the concentration is observed here for the increase of Soret number (Sr) and chemical reaction parameter (γ).

In the figure 13, the variation of concentration, with the simultaneous increase of the Prandtl number (Pr) and permeability parameter (K), is shown. The effect of permeability parameter is to decrease the concentration since with the increase of permeability, the fluid becomes thinner but with the simultaneous increase of Prandtl number, the concentration increases. Prandtl number increases the viscosity which in turn increases the concentration.

Graphical results of concentration profiles for different values of Schmidt number Sc and chemical reaction parameter (γ) are shown in Figure14. The figure shows that an increase in Sc, decreases the concentration. Further more, it is interesting to note that the concentration profiles fall slowly and steadily for Hydrogen (Sc~0:2) and Helium (Sc~0:3) but falls very rapidly for water vapour (Sc~0:6). Physically this is true because of the fact that the water vapour can be used for maintaining normal concentration field where as Hydrogen can be used for maintaining effective concentration field. The physical effect of chemical reaction parameter (γ) clearly demonstrates that concentration profiles decrease rapidly when γ is increased.

Figures 15.1 and 15.2are plotted to show the comparative study of the dimensionless time t on the concentration when $\Pr = 0.71$ and $N = 1$ and $Sc = 2$ and $\gamma = 1$ Four different values of time $t \cong 0.4,\ 0.6,\ 0.8,$ and 1.0 are chosen. We

found that the concentration increases when the time (t) is increased.

The variation of concentration distribution with the physical parameters Schmidt number (Sc) and the chemical reaction parameter (γ) is observed from the figure 16. With the increase of Sc and γ, the velocity decreases gradually in the boundary layer and reaches a steady state. This effect can be seen from the figure.

The effects of Soret and Eckert numbers on the concentration distribution are plotted in the figures 17 and 18. As the Soret number increases the concentration increases in the middle of the boundary layer but eventually decreases. This can be observed from the figure 17. The gradual thinning of the fluid in the boundary layer with the increase of Eckert number (Ec) is showed in the figure 18.

Table-I Variation in Skin-friction coefficient(τ)

M	γ	Gr	Gc	Pr	K	Sc	a	τ(Skin-friction)
5	1	1	1	0.71	0.1	0.22	$-\pi/6$	-2.273828
10	1	1	1	0.71	0.1	0.22	$-\pi/6$	-3.126577
5	3	1	1	0.71	0.1	0.22	$-\pi/6$	-2.491116
5	1	3	1	0.71	0.1	0.22	$-\pi/6$	-1.853089
5	1	1	4	0.71	0.1	0.22	$-\pi/6$	-1.958154
5	1	1	1	1	0.1	0.22	$-\pi/6$	-2.384553
5	1	1	1	0.71	0.5	0.22	$-\pi/6$	-2.672829
5	1	1	1	0.71	0.1	0.60	$-\pi/6$	-2.491116
5	1	1	1	0.71	0.1	0.22	$\pi/6$	-1.60452

The skin–friction coefficient at the wall (τ) is given in the tables I. It is clearly noticed that the increase in magnetic field (M), permeability parameter (K), Solutal Grashof number (Gc) and Prandtl number (Pr) causes the decrease in Skin-friction coefficient. The shear stress increases with the increasing values of the chemical reaction parameter (γ), thermal Grashof number (Gr), Schmidt number (Sc) and the inclination of the plate(α) . But for constant values ofEc,Nand.t.

Table II Variation of rate of heat transfer (Nu)

M	γ	Gr	Gc	Pr	K	Sc	N	t	Ec	α	Nu
5	1	1	1	0.71	0.1	0.22	1	0.4	1	$-\pi/6$	-.8215216
10	1	1	1	0.71	0.1	0.22	1	0.4	1	$-\pi/6$	-.7780302
5	3	1	1	0.71	0.1	0.22	1	0.4	1	$-\pi/6$	-.480635
5	1	3	1	0.71	0.1	0.22	1	0.4	1	$-\pi/6$	-.9846448
5	1	1	4	0.71	0.1	0.22	1	0.4	1	$-\pi/6$	-.4840673
5	1	1	1	1	0.1	0.22	1	0.4	1	$-\pi/6$	-.4738897
5	1	1	1	0.71	0.5	0.22	1	0.4	1	$-\pi/6$	-.471469
5	1	1	1	0.71	0.1	0.60	1	0.4	1	$-\pi/6$	-.9806249
5	1	1	1	0.71	0.1	0.22	2	0.4	1	$-\pi/6$	-2.404324
5	1	1	1	0.71	0.1	0.22	1	0.6	1	$-\pi/6$	-.5711901
5	1	1	1	0.71	0.1	0.22	1	0.4	3	$-\pi/6$	-.418885
5	1	1	1	0.71	0.1	0.22	1	0.4	1	$\pi/6$	-.8062888

The table III gives the variation of rate of heat transfer in terms of Nusselt number. With the increase of magnetic field (M), Solutal Grashof number(Gc), Chemical reaction parameter (γ),Prandtl number (Pr), Permeability parameter(K),time t and Eckert number (Ec) causes the increase in the Nusselt number. The Nusselt number decreases with increase in thermal Grashof number (Gr), Schmidt number (Sc), N and inclination of the plate (α).

Table III Variation of rate of mass transfer (Sh)

M	γ	Gr	Gc	Pr	K	Sc	N	t	Ec	a	Sh(Sherwood number)
5	1	1	1	0.71	0.1	0.22	1	0.4	1	$-\pi/6$	-1.981967
10	1	1	1	0.71	0.1	0.22	1	0.4	1	$-\pi/6$	-2.025409
5	3	1	1	0.71	0.1	0.22	1	0.4	1	$-\pi/6$	-.6178092
5	1	3	1	0.71	0.1	0.22	1	0.4	1	$-\pi/6$	-1.073927
5	1	1	4	0.71	0.1	0.22	1	0.4	1	$-\pi/6$	-.6082868
5	1	1	1	1	0.1	0.22	1	0.4	1	$-\pi/6$	-.6122832
5	1	1	1	0.71	0.5	0.22	1	0.4	1	$-\pi/6$	-.5392113
5	1	1	1	0.71	0.1	0.60	1	0.4	1	$-\pi/6$	-1.381791
5	1	1	1	0.71	0.1	0.22	2	0.4	1	$-\pi/6$	-1.973262
5	1	1	1	0.71	0.1	0.22	1	0.6	1	$-\pi/6$	-1.114278
5	1	1	1	0.71	0.1	0.22	1	0.4	3	$-\pi/6$	-2.332864
5	1	1	1	0.71	0.1	0.22	1	0.4	1	$\pi/6$	-1.997039

From the table III, it is observed that with the increase of the magnetic field (M), Eckert number (Ec), thermal Grashof number (Gr), Prandtl number (Pr)and Schmidt number (Sc) leads to decrease in Sherwood number. the inclination of the plate, the rate of mass transfer increases with the increase of chemical reaction parameter (γ), Solutal Grashof number (Gc), Permeability parameter (K), time t and inclination of the plate (α).

Particular cases

The following published results are reduced as special cases from the present solutions.

1. The results obtained in the absence of viscosity, thermal and mass transfer effects are quite identical to the known result obtained bySamiulhaqet.al [13] for $\omega \to 0$ the impulsive motion of the plate. Furthermore, the solution corresponding to hydrodynamic fluid passing through a non - porous medium is obtained by neglecting the magnetic and porous effects.
2. In the absence of variable mass diffusion and when $Sr = 0$ the results are similar with the results of Muthucumaraswamy R, Janakiraman B[17].
3. In the absence of radiation, viscous and mass diffusion and, the solutions through the non–porous medium, obtained were in agreement with the results of Rajput and Kumar (9).

V. Conclusions

An analysis of combined effects of Soret and Chemical reaction on the radiative MHD free convective flow of an electrically conducting incompressible viscous fluid over an inclined plate embedded in a porous medium is considered. The dimensionless momentum equation coupled with the energy and mass diffusion equations are numerically solved. The effects of pertinent parameters on velocity, temperature and concentration are graphically displayed where as the

variations in skin friction, Nusselt number and Sherwood number are presented through tables. we conclude that

1. The velocity profiles increases with increase in Gr, Gr &Gc, Pr &K, Sc &γ and decrease with increase in M, Gr<0 and α.
2. Temperature profiles increases with increase in t & Ec and decrease with increase in Pr& K, and Pr& N.
3. Increase in Sr&γ,Sc&γ,Ec leads to decrease in concentration profiles and increase in Sr, Sc &t causes increase in concentration profiles.
4. With an increase in M, Gc, Pr and K tends to decrease in Skin-friction while increase in γ, Gr, αSc and leads to increase in Skin-friction.
5. Increase in M, Gc, Pr, K,t, Ec and γ causes decrease in Nusselt number and Increase in Gr, Sc, N and α leads to decrease in Nusselt number.
6. The Sherwood number increases with increase in Gc, K, t, γ and α while decease with increase in M, Gr, Pr, Sc, N and Ec.
7. The results obtained in the absence of viscosity, thermal and mass transfer effects are quite identical to the known result obtained by Samiulhaq et al. [13] for $\omega \to 0$ the impulsive motion of the plate. Furthermore, the solution corresponding to hydrodynamic fluid passing through a non - porous medium is obtained by neglecting the magnetic and porous effects.
8. In the absence of variable mass diffusion and when $Sr = 0$ the results are coincides with the results of Muthucumaraswamy R, Janakiraman B[17].
9. In the absence of radiation, viscous and mass diffusion and, the solutions through the non – porous medium, obtained were in agreement with the results of Rajput and Kumar [9].

REFERENCES

[1] Guo Z and Sung Hj, Conjugate Heat and Mass transfer in metal hydride beds in the hydriding process, *Int. J. of Heat Mass Transfer*, 42, P379 – 382, 1999.

[2] Cheng Cy, Natural heat and mass transfer from a sphere in micro polar fluids with constant wall temperature and concentration, *Int. Comm.Heat Mass Transfer*, 35, P750-755, 2008.

[3] Muthucumaraswamy R, Ravi Shankar M, First order chemical reaction on isothermal vertical oscillating plate with variable mass diffusion isothermal infinite vertical plate, *Ind. J. of Sci. and Tech.*, 4, P573-577, 2011.

[4] Narahari M. Bég OA, Ghosh S.K., Mathematical modeling of mass transfer and free convection current effects on unsteady viscous flow with ramped wall temperature, *World J. Mech.*,1, P176 – 184, 2011.

[5] Cramer K.R, Pai S.I. *Magneto fluid dynamics for Engineers and Applied Physicists*, McGraw - Hill Book Company, New York.

[6] Bhuvanseswari M, Sivasankaran S, Kim YJ, Exact analysis of radiation convective flow heat and mass transfer over an inclined plate in a porous medium, *World Ap.Sci. J*, 10,P774–778, 2010.

[7] Kandasamy R, Muhaimin I, Salim H, Lie group analysis for the effect of temperature – dependent fluid viscosity with thermophoresis and chemical reaction on MHD free convective heat and mass transfer overa porous stretching surface in the presence of heat source / sink, *Comm. Nonlinear Sci. Num. Simul*, 15, P2109–2123, 2010.

[8] Ahmed N, Sarmah HK, Thermal radiation effect on a transient MHD flow with mass transfer past an impulsively fixed infinite vertical plate, *Int. J. Appl. Math.Mech*, 5,P87–98, 2009.

[9] Rajput US, Kumar S, MHD flow past an impulsively started vertical plate with variable heat and mass diffusion, Appl. Math. Sci, 5, P149–157, 2012.

[10] Rajput US, Kumar S, Radiation effects on MHD flow past an impulsively started vertical plate with variable heat and mass transfer, *Int. J. Appl. Math. Mech*, 8, P66–85, 2012.

[11] Ahmad N, Soret and radiation effects on transient MHD free convection from an impulsively started infinite vertical plate, *J Heat Transfer*, 134, 2012.

[12] Osman ANA, Abo-Dahab SM, Mohamed RA, Analytical solution of thermal radiation and chemical reaction effects on unsteady MHD convection through porous media with heat source / sink, *Math. Prob. Engg.*, P1–18, 2011.

[13] Samiulhaq, Fetecau C, Khan I, Ali F, Shafie S, Radiation and porosity effects on the MHD flow past an oscillating vertical plate with uniform heat flux, *Z. Naturforsch*, 67a, P572–580, 2012.

[14] Samiulhaq, Khan I, Ali F, Shafie S, MHD free convection flow in a porous medium with thermal diffusion and ramped wall temperature, *J. Phys. Soc.Jpn*, 81, 2012.

[15] Magyari E, Pantokratoras A, Note on the effect of thermal radiation in the linearized Rosseland's approximation on the heat transfer characteristics of various boundary layer flows, *Int. Comm. Heat Mass Transfer*, 38, P554–556, 2011.

[16] Ziyauddin, Kumar M, Radiation effect on unsteady MHD heat and mass transfer flow on a moving inclined porous heated plate in the presence of chemical reaction, *Int J Math Modell Simul. Appl*, 3, P155–163, 2010.

[17] Muthucumaraswamy R, JanakiramanB, MHD and radiation effects on moving isothermal vertical plate with variable mass diffusion, *Theo. Appl. Mech*, 33, P17–29, 2006.

[18] Farhad Ali, Ilyas Khan, Samiulhaq, SharidanShafle, Conjugate effects of heat and mass transfer on MHD

a. Freeconvection flow over an inclined plate embeddedin a porous medium,*PLOS ONE | www.plosone.org*, 8, 6, e65223, 2013

M.Rajaiah presently working professor an HOD department of Humanities and Sciences ,Audisankara College of Engineering &Technology ,Gudur, Nellore, AP, India.I have 17 years of extensive experience in teaching various disciplines like M.Sc., M.Tech and B.Tech etc.I published three research papers and presented two papers on International Conferences. Board of Studies Chairman for Engineering Mathematics, Engineering Physics, Engineering Chemistry, Environmental Studies and Communicative English in Audisankara College of Engineering & Technology, Gudur, SPSR Nellore. Best Professor & HOD Award in the year 2008 From Late Dr.Y.S.Rajasekhar Reddy Former Chief Minister of Andhrapradesh for getting good results Overall Andhrapradesh JNTU Engineering Colleges.